# High-resolution Functional Magnetic Resonance Imaging Reveals Configural Processing of Cars in Right Anterior Fusiform Face Area of Car Experts

**David A. Ross[1], Benjamin J. Tamber-Rosenau[2,3], Thomas J. Palmeri[2], JieDong Zhang[4], Yaoda Xu[4], and Isabel Gauthier[2]**

## Abstract

■ Visual object expertise correlates with neural selectivity in the fusiform face area (FFA). Although behavioral studies suggest that visual expertise is associated with increased use of holistic and configural information, little is known about the nature of the supporting neural representations. Using high-resolution 7-T functional magnetic resonance imaging, we recorded the multivoxel activation patterns elicited by whole cars, configurally disrupted cars, and car parts in individuals with a wide range of car expertise. A probabilistic support vector machine classifier was trained to differentiate activation patterns elicited by whole car images from activation patterns elicited by misconfigured car images. The classifier was then used to classify new combined activation patterns that were created by averaging activation patterns elicited by individually presented top and bottom car parts. In line with the idea that the configuration of parts is critical to expert visual perception, car expertise was negatively associated with the probability of a combined activation pattern being classified as a whole car in the right anterior FFA, a region critical to vision for categories of expertise. Thus, just as found for faces in normal observers, the neural representation of cars in right anterior FFA is more holistic for car experts than car novices, consistent with common mechanisms of neural selectivity for faces and other objects of expertise in this area. ■

Downloaded from http://direct.mit.edu/jocn/article-pdf/30/7/973/1787628/jocn_a_01256.pdf by guest on 20 September 2021

## INTRODUCTION

Expertise in identifying visually similar objects is associated with category-selective responses in the fusiform face area (FFA; e.g., Gauthier, Skudlarski, Gore, & Anderson, 2000). Correlations between behavioral performance in visual tasks and FFA selectivity have been shown for many categories, such as faces (Elbich & Scherf, 2017; McGugin, Ryan, Tamber-Rosenau, & Gauthier, 2017), cars (McGugin, Gatenby, Gore, & Gauthier, 2012), birds (Gauthier et al., 2000), radiographs (Bilalić, Grottenthaler, Nägele, & Lindig, 2016), and chess configurations (Bilalić, Langner, Ulrich, & Grodd, 2011).[1]

Although visual expertise is often associated with category-selective responses in FFA, category-selective responses do not guarantee good performance with an object category. For example, individuals with developmental prosopagnosia, who by definition have seriously impaired face recognition, have seemingly normal face-selective responses in FFA (Avidan et al., 2014; Furl, Garrido, Dolan, Driver, & Duchaine, 2011). Addressing this apparent contradiction, a study using multivariate pattern analysis (MVPA) revealed that the FFA response to faces in these patients is not normal (Zhang, Liu, & Xu, 2015). In typical individuals, the response pattern across FFA voxels can distinguish between a normal face and a misconfigured face, in which the top and bottom parts have been switched. Interestingly, for individuals with developmental prosopagnosia, this gross configural change does not affect the response pattern in FFA (see also Schiltz, Dricot, Goebel, & Rossion, 2010; Schiltz et al., 2006). This finding is consistent with reports of abnormal configural and holistic processing in individuals with prosopagnosia (Liu & Behrmann, 2014; Marotta, McKeeff, & Behrmann, 2002) and suggests that the sensitivity of FFA response patterns to configuration may predict expert performance better than mere selectivity.

The question therefore arises: In a nonface domain of expertise, would the response of the FFA depend on configuration or would it be selective regardless of configuration as it is for faces with prosopagnosic patients? If responses to nonface objects in FFA arise for reasons similar to the face responses, then they should be equally dependent on configuration. Specifically, here, we predict that expertise with cars should be associated with sensitivity to the configuration of car parts in FFA, whereas car novices would show less such sensitivity; although FFA representations may not have any sensitivity to configuration in prosopagnosic patients, we would not go as far as equating being a car novice to having a face recognition impairment. There is some indication that

[1]University of Massachusetts Amherst, [2]Vanderbilt University, [3]University of Houston, [4]Harvard University

© 2018 Massachusetts Institute of Technology

perceptual expertise can increase configural processing. Training with novel objects produces holistic processing, demonstrated by a failure to selectively attend among the available object parts despite task demands to do so, effects that are sensitive to configuration (Chua, Richler, & Gauthier, 2015; Wong, Palmeri, & Gauthier, 2009; Gauthier & Tarr, 2002; Gauthier, Williams, Tarr, & Tanaka, 1998). Moreover, car experts process cars holistically only when car parts are in a normal configuration (Bukach et al., 2010; Gauthier, Curran, Curby, & Collins, 2003). Studies have reported correlations between fusiform gyrus selectivity for trained objects and holistic processing of these objects in their trained configuration (Wong, Palmeri, & Gauthier, 2009; Gauthier & Tarr, 2002). Yet, no direct measurement of sensitivity to configuration in neural responses evoked by nonface objects in real-world expertise has been conducted.

Here, we ask whether car expertise predicts how well multivoxel response patterns in FFA discriminate configural changes in car parts. We first sought to replicate standard expertise effects, measuring car selectivity in posterior and anterior FFA (FFA1 and FFA2, respectively), occipital face area (OFA), and lateral occipital complex (LO), expecting car expertise to correlate with car selectivity. Note that, in previous work, car expertise has predicted selective responses to cars in both face-selective and non-face-selective areas (McGugin, Gatenby, Gore, & Gauthier, 2012; Harel, Gilaie-Dotan, Malach, & Bentin, 2010), but effects in many of these areas disappeared with increased attentional and perceptual loads, leaving a robust correlation between car expertise and neural selectivity only in the right FFA2 (rFFA2; McGugin, Newton, Gore, & Gauthier, 2014). Other studies found stronger effects of experience or expertise in FFA2 (Golarai, Liberman, & Grill-Spector, 2017; McGugin et al., 2017; McGugin, Van Gulick, et al., 2014). Accordingly, we expect that most of our ROIs may show an effect of car expertise (as measured here in a low-demand 1-back task) but that the rFFA2 may be the main region that is sensitive to configuration of car parts as a function of car expertise.

To test this hypothesis, we measured BOLD functional magnetic resonance imaging (fMRI) activity patterns while participants viewed images of intact cars, misconfigured cars (location of the top and bottom parts exchanged), and individually presented top and bottom car parts. To assess whether car representations were sensitive to configuration, we trained a support vector machine (SVM) classifier to differentiate the multivoxel patterns elicited by whole and configurally disrupted cars in each ROI. For each participant, we asked the SVM to quantify the similarity of a combined linear combination of the voxel pattern elicited by separate top and bottom car parts to either the pattern elicited by whole cars or the pattern elicited by configurally disrupted cars. On the basis of prior work (MacEvoy & Epstein, 2011), we used an equal combination of the patterns elicited by each part. We expect that, in car novices, cars would be represented in a part-based manner and so a combination of parts would be roughly equally similar to whole cars and to misconfigured cars. Prior work shows that expertise effects with cars are reduced when the configuration of halves is disrupted (e.g., Bukach et al., 2010; Gauthier et al., 2003). Accordingly, we expect that car representations should become increasingly sensitive to configuration as a function of car expertise and that the combined pattern, which cannot carry information about whole car configuration, should look less like the patterns elicited by whole cars and consequently more like the patterns elicited by misconfigured cars.

## METHODS

### Participants

Thirty men with normal or corrected-to-normal vision were recruited for this experiment, with two participants excluded from further analyses for failure to comply with instructions during behavioral testing (remaining participants: $M = 24.6$ years old, $SD = 5.5$ years). A deliberate effort was made to recruit participants with a broad range of car expertise, although all our participants, even novices, are expected to have some experience with car models. This was effective in increasing variability especially at the high end of the spectrum of ability. In a sample of 213 participants not recruited for expertise with any category (Van Gulick, McGugin, & Gauthier, 2016), the mean (standard deviation) for the VETcar (see description below) was 0.60 (0.14). The present sample has a mean of 0.69 (0.21), with no participant falling 2 *SD*s below the mean but six participants (20%) falling 2 *SD*s above the mean. The sample size was based on an expected effect size of $r = .5$ for car expertise correlations with FFA activity (McGugin, Van Gulick, et al., 2014), which requires a sample size of 26 participants for 80% power at an alpha of .05. Participants took part in the study for monetary compensation, and written informed consent was obtained in accordance with a protocol approved by the Vanderbilt institutional review board.

### Behavioral Tests and Stimuli

All participants completed a sequential matching task (e.g., Gauthier et al., 2000), a Vanderbilt Expertise Test (VET) battery (McGugin, Van Gulick, et al., 2014; McGugin, Richler, Herzmann, Speegle, & Gauthier, 2012), and the Cambridge Face Memory Test (CFMT; Duchaine & Nakayama, 2006).

The stimuli for the sequential matching task were images of birds, cars or planes. On each trial, participants judged if two sequentially presented images showed the same object (same make and model of car or airplane or same species of bird) or not; images were always

Downloaded from http://direct.mit.edu/jocn/article-pdf/30/7/973/1787628/jocn_a_01256.pdf by guest on 20 September 2021

different. The first stimulus of each pair was displayed for 1000 msec, followed by a 500-msec mask. The second stimulus was then displayed until a response was made (up to a maximum of 5000 msec). Trials were blocked by object category.

The VET battery included eight separate tests for eight different categories: leaves, owls, butterflies, wading birds, mushrooms, cars, planes, and motorcycles (see McGugin, Richler, et al., 2012, for details). For each category, participants first studied a set of six images, with each image showing a different species/model from the test category. This was followed by 48 three-alternative forced choice trials comprising a target image of one of the six studied species/models and two foil images of unstudied species/models from the test category. For the first 12 trials of each block, the target image was an exact match to one of the six studied images, whereas for the remaining 36 trials, it was a new image matching the identity of one of the six studied species/models (new target/foil images were used for each test trial).

In the CFMT (Russell, Duchaine, & Nakayama, 2009; Duchaine & Nakayama, 2006), participants studied frontal views of six target faces, followed by a short learning phase in which the participants saw cartoon faces to familiarize them with the task. Participants were then presented with 54 three-alternative forced choice test trials containing one target face and two distractor faces. Matching faces varied in lighting, pose, or both relative to their studied presentation. In addition, the final 24 trials were presented with faces embedded in Gaussian noise to increase difficulty level.

## Structural MRI and fMRI

Imaging was performed using a Philips Achieva 7-T human MRI scanner located in the Vanderbilt University Institute of Imaging Science. All scanning was performed using a 32-channel SENSE parallel-imaging head coil. Functional scanning used EPI protocols. All participants completed a single scanning session consisting of a structural scan, a standard-resolution localizer, a high-resolution localizer, and six to eight high-resolution experimental runs. We used the IView Bold analysis package provided by Philips to place the high-resolution slices for each participant so that they included the FFA1 and FFA2 identified during the standard-resolution scan.

### *Structural Scan*

Structural T1 scans were acquired using 249 0.7-mm sagittal slices with a 352 × 351 matrix covering a field of view of 246 × 246 mm, for a final isotropic resolution of 0.7 mm. Structural scans used a repetition time (TR) of 4.761 msec, a flip angle of 7°, and an echo time (TE) of 2.1 msec.

### *Standard-resolution Functional Localizer*

Standard-resolution functional scans covering nearly the whole brain were acquired to define our functional ROIs. These scans used a 3-D PRESTO sequence covering a volume of 211 × 211 × 85 mm. Functional volumes were reconstructed into 34 2.5-mm axial–oblique slices with a 96 × 96 matrix for a final in-plane resolution of 2.198 × 2.198 mm. Standard-resolution scans used a volume acquisition time of 2 sec, a TR of 15.16 msec, a flip angle of 12°, and a TE of 20.06 msec. After preprocessing, standard-resolution scans were resampled to an isotropic resolution of 3 mm. Standard-resolution localizer scans consisted of 256 volumes (512 sec). In addition to the standard processing pipeline, un-resampled standard-resolution functional localizer scans were analyzed in real time using IView to aid in placement of high-resolution slices (see below).

During the localizer, participants completed a 1-back repetition task while viewing blocks of faces, objects, body parts, and scrambled objects. Each block was composed of 16 images from one of the four categories, with eight blocks of each category (4 categories × 8 blocks). Stimuli were drawn from a pool of grayscale photographs of 36 male and female white adult faces; 36 images of common household objects; 206 body-part images, including whole bodies (without heads) and individual limbs, hands, and feet; and 40 scrambled images, created by dividing a separate set of images of airplanes into squares and scrambling their locations. Each stimulus appeared on screen for 1 sec, and no two consecutive stimuli were of the same size. Repeats occurred one to two times per block, and participants were instructed to press a button only for immediate repetitions.

### *High-resolution Functional Localizer*

High-resolution functional scans were acquired to verify category selectivity and effects of expertise in functional ROIs. These scans used EPI with 32 contiguous 1.5-mm axial–oblique slices placed to cover regions initially localized using the standard-resolution functional scans with real-time analysis. Volume TR was 4 sec, flip angle was 65°, and TE was 25 msec. These scans were acquired with a 148 × 145 matrix covering a field of view of 224 × 224 mm and were reconstructed using a 160 × 160 matrix for a final in-plane acquisition resolution of 1.4 × 1.4 mm. After preprocessing, high-resolution scans were resampled to an isotropic resolution of 1 mm. High-resolution localizer scans consisted of 80 volumes (320 sec). Because of the limited brain coverage necessitated by high-resolution imaging and the individualized slice placement to target ROIs identified in IView during the standard-resolution localizer, high-resolution coverage varied across participants. For coverage to include the targeted ROIs, we placed the slice stack such that it missed the anterior

Downloaded from http://direct.mit.edu/jocn/article-pdf/30/7/973/1787628/jocn_a_01256.pdf by guest on 20 September 2021

temporal poles, the occipital pole, and the frontal pole in most participants.

During the high-resolution localizer, participants completed a 1-back repetition task while viewing blocks of faces, objects, cars, and scrambled objects. Each block was composed of 16 images from one of the four categories, with five blocks of each category (4 categories × 5 blocks). Stimuli were drawn from a pool of 40 grayscale photographs of white male faces as well as 70 car images. The car images were from modern car models and did not overlap with the images used in the experimental task. The stimulus presentation and task instructions were the same as in the standard-resolution localizer.

### *High-resolution Functional Experimental Task*

Experimental task scans were acquired to test our predictions about configural sensitivity using multivoxel pattern analysis. The slice placement and scanning parameters were the same as for the high-resolution functional localizer scans, except that each task scan consisted of 50 volumes (200 sec). In each experimental run, participants completed a motion detection task comprising eight blocks of 20 images. The images in each block came from one of four conditions—whole car images, misconfigured car images, isolated top car-part images, or isolated bottom car-part images—with two blocks of each stimulus condition per run. Task blocks were interleaved between 8-sec fixation blocks with each run beginning and ending with fixation. Each task block contained 20 images, each presented for 600 msec and followed by a 200-msec blank interval. For the duration of each run, participants were instructed to fixate on a dot in the center of the screen. To engage their attention, a randomly selected four images in each block moved 5 pixels to the left or to the right during stimulus presentation. Participants were asked to indicate the direction of these movements by a button press. For the intact and configurally disrupted images, the movement would occur on either the upper or lower part to encourage the participants to attend equally to both parts of the images. All but three of the participants completed eight blocks of the task, with two completing seven blocks and one completing six blocks.

The car images were grayscale and showed a three-quarter front view of a car facing to the right. Each car image was divided into two parts, with a box surrounding each part. The top part contained the roof and windows, and the bottom part contained the wheels and most of the body of the car. Each car image was used to create one of the four stimulus types (see Figure 1): whole cars, in which the top and bottom were presented in the correct configuration; misconfigured cars, in which the top and bottom halves were switched; and isolated top and bottom car halves. The sizes of the upper and lower car parts on the screen were 1.9° × 14.5° and 2.9° × 14.5°, respectively. The intact and misconfigured car images were simply the vertical combination of the two parts (i.e., 4.8° × 14.5°). All images were presented centered on a fixation dot located in the center of the screen.

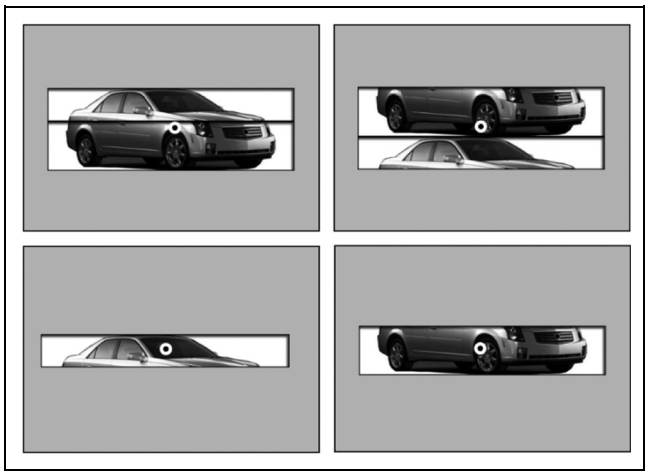

**Figure 1.** Example of car images used in the main experimental task. Top left: whole car, top right: configurally disrupted car, bottom left: top car part, and bottom right: bottom car part.

Because our goal was to predict decoding as a function of car expertise rather than to decode location, we presented car parts at fovea rather than in their original positions in whole images. We do not expect that the positioning of these parts could drive SVM decoding because the population receptive fields of voxels in FFA have a median size of 3.4° when stimuli are attended (Kay, Weiner, & Grill-Spector, 2015), and our parts were displaced a maximum of 1.5°. In addition, the parts overlapped by 50% in their location across the whole and part conditions, further suggesting that they should engage largely overlapping cell populations. Finally, we focus here on the relative effects across participants, not expected to interact with receptive field effects.

## Data Analyses

### *Behavioral Data*

For each participant, $d'$ scores were calculated for each category in the sequential matching task (bird, car, and plane) and percent correct scores were calculated on the CFMT and for each category on the VET (butterflies, cars, leaves, motorcycles, mushrooms, owls, planes, and wading birds). Aggregate car task scores were computed as the mean of the $z$-transformed scores for cars on the sequential matching task and VET. To obtain an aggregate measure of car-specific expertise, we used the nonvehicle categories of the matching task and VET (birds, leaves, owls, butterflies, wading birds, and mushrooms) as a baseline, computed nonvehicle aggregate scores, and regressed them out of the car aggregate scores.[2] We used only the nonvehicle categories to control for general object recognition because, as in McGugin, Richler,

Downloaded from http://direct.mit.edu/jocn/article-pdf/30/7/973/1787628/jocn_a_01256.pdf by guest on 20 September 2021

et al. (2012), performance with cars was highly correlated with performance on the other two vehicle categories (planes and motorcycles); this is likely because of joint experience and interest. For the sequential matching task, performance on car trials was correlated with performance on plane trials, $r = .67$, $p = .0001$, and for the VET, performance on car trials was correlated with performance on motorcycle trials, $r = .63$, $p = .0003$, and marginally significant with performance on plane trials, $r = .37$, $p = .0542$. In the remainder of this article, we simply refer to residualized car aggregate scores as "car expertise."

### *Functional Data*

The functional data were analyzed using BrainVoyager, in-house MATLAB code written using the NeuroElf toolbox (neuroelf.net), and LibSVM (Chang & Lin, 2011). High-resolution T1 scans were used for registering the functional scans and calculating Talairach warping parameters. Functional scan preprocessing in BrainVoyager included slice acquisition time correction (high-resolution EPI scans only), 3-D motion correction, linear trend removal, and temporal high-pass filtering (three cycles per run). The data from all high-resolution runs were interpolated to 1-mm isotropic space and warped to Talairach space (Talairach & Tournoux, 1988). Standard- and high-resolution localizer runs (used in the univariate analyses) were spatially smoothed, which is considered optimal for detection purposes (Worsley, Evans, Marrett, & Neelin, 1992), with a 6-mm Gaussian kernel, but experimental task runs (used in the multivariate analyses) were left unsmoothed.

### *Standard-resolution Functional Localizer*

To identify FFA1, FFA2, OFA, and LO, we ran separate general linear models for each participant, with regressors for faces, body parts, objects, and scrambled objects, on the standard-resolution localizer runs (Friston, Frith, Turner, & Frackowiak, 1995). The individual-participant centers of FFA1, FFA2, and OFA were defined by the peaks of the contrast faces minus objects ($t$ test, $p < .05$) in middle fusiform (posterior: FFA1, anterior: FFA2) and inferior occipital cortex, respectively. The center of LO was defined by the peak activation of the contrast objects minus scrambled objects in the lateral occipital cortex ($t$ test, $p < .05$). An additional "body parts minus objects" contrast was used to help distinguish FFA1 and FFA2, which are typically separated by a body-part-selective area (Weiner & Grill-Spector, 2010). We aimed to create ROIs that were equal in size (to yield comparable sensitivity for MVPA) and that were sufficiently large for MVPA (Kriegeskorte, Goebel, & Bandettini, 2006). ROI size varies slightly because voxels that were initially included in more than one ROI were excluded from all ROIs, as were voxels with a raw BOLD signal value of less than 20, which excludes voxels that clearly fall outside the brain. To standardize the spatial extent of our ROIs across participants, we defined ROIs as spheres (radius = 7.5 mm) centered on the peak $t$ value for each contrast. Talairach coordinates, size, and number of individuals are reported in Table 1. Final ROI size was not correlated with car expertise ($r$s $< .15$, $p$s $> .49$).

### *High-resolution Functional Localizer*

The high-resolution functional localizer runs were similarly subjected to a general linear model analysis (with regressors for face, car, object, and scrambled object blocks) to extract parameter (beta) weights and measure the relationship between car expertise and univariate face and car selectivity in each individual participant ROI.

### *High-resolution Experimental Task*

The data from the experimental task runs were analyzed using a linear probabilistic SVM trained and tested on the multivoxel activation patterns within each ROI (Chang

**Table 1.** ROI Descriptions (Mean Talairach Coordinates, Number of Participants with a Given ROI, and ROI Mean Size, Corresponding to the Number of 1-mm Isotropic High-resolution Voxels)

| *ROI* | *x (SD)* | *y (SD)* | *z (SD)* | *N* | *ROI Size (SD)* |
|---|---|---|---|---|---|
| Left FFA1 | −39.0 (5.8) | −62.8 (8.2) | −21.0 (4.8) | 20 | 1665 (302) |
| Left FFA2 | −40.4 (5.7) | −45.4 (6.2) | −23.0 (5.7) | 22 | 1668 (345) |
| Left OFA | −39.5 (6.6) | −81.6 (6.4) | −19.1 (4.1) | 17 | 1513 (463) |
| Left LO | −45.6 (7.1) | −76.0 (8.5) | −14.3 (8.8) | 24 | 1792 (0) |
| rFFA1 | 38.1 (6.4) | −66.0 (9.9) | −17.1 (4.0) | 21 | 1555 (378) |
| rFFA2 | 38.6 (4.1) | −46.4 (5.6) | −22.6 (3.5) | 21 | 1738 (229) |
| Right OFA | 34.4 (5.4) | −84.0 (6.9) | −16.3 (4.3) | 21 | 1623 (269) |
| Right LO | 44.6 (5.5) | −75.8 (6.7) | −13.4 (7.3) | 27 | 1792 (0) |

Downloaded from http://direct.mit.edu/jocn/article-pdf/30/7/973/1787628/jocn_a_01256.pdf by guest on 20 September 2021

& Lin, 2011). For each ROI, the pattern of BOLD activation across voxels at each time point was extracted and *z* scored. For each 16-sec block (i.e., four TRs), a mean activation pattern was computed for the 16-sec period beginning 4 sec after block onset and ending 20 sec after block onset (i.e., offset forward in time by one TR). We first trained and then tested an SVM to estimate the probability that a given activation pattern belonged to a whole car block versus a misconfigured car block, using leave-one-block-out cross-validation to ensure independence of training and test data. That is, the SVM yielded a single probability for each test pattern representing the evidence that the pattern belonged to a whole car block. Note that, because the choice of target category is not important (i.e., a .8 probability that a test pattern belonged to a whole car block implies a .2 probability that it belonged to a misconfigured car block), we combined the SVM probabilities for whole and misconfigured car-pattern classifications by taking 1 minus the classification probability on misconfigured car-pattern test trials and calculating the mean probability correct (Table 4). Next, we sought to investigate if the combined activation patterns (averaged top- and bottom-only activation patterns) were equally similar to activation patterns elicited by whole and misconfigured cars (consistent with parts-based representation) or were more similar to activation patterns elicited by whole cars than misconfigured cars (consistent with holistic representation). Thus, we trained the probabilistic SVM using the full set of activation patterns from whole and configurally disrupted car blocks and tested it on combined activation patterns, using the probability estimates as an index of similarity. Combined activation patterns were created by exhaustively pairing the 16 activation patterns from the top and bottom car-part blocks and computing the mean activation in each voxel.

## RESULTS

### Univariate Analyses: Expertise Effects in Car Selectivity

First, we sought to replicate prior work demonstrating expertise effects in ventral occipito-temporal cortex (McGugin, Newton, et al., 2014; McGugin, Van Gulick, et al., 2014; McGugin, Gatenby, et al., 2012; Xu, 2005; Gauthier et al., 2000). To maximize our power, given that several studies have reported expertise effects in these ROIs and because we have a clear directional prediction, we report one-tailed tests for positive correlations. We do not correct for multiple comparisons and invite readers to treat *r* values as estimates of effect size. In the ROIs defined in the standard-resolution localizer, we measured the univariate response to cars (beta weights) relative to the average for the noncar conditions (faces, scrambled objects, objects) in the high-resolution localizer. Because most fMRI studies of car expertise have subtracted neural activity for noncar conditions from the neural response to cars, we report correlations of car expertise with a subtracted score. Because partialing out activity for noncars from the response to cars is arguably a better approach (so that the noncar variance does not contribute to the correlation with behavior), we also report partial correlations between car expertise and car residuals (neural activity for cars, regressing out neural activity for noncars). The two methods are generally consistent and show significant or near-significant car expertise effects in most areas, with the exception of left OFA and right FFA1 (rFFA1; see Table 2). Because we also collected CFMT scores, we report similar analyses for faces, relating CFMT performance to either neural activity for faces either subtracting the three nonface conditions or partialing them out. As in other work (McGugin et al., 2017), face recognition behavior does not show robust correlations with neural selectivity for faces in most ROIs. This may be due to the greater variation in both behavior and neural activity for cars than faces in our sample of

**Table 2.** Univariate Expertise Effects

*A. Pearson Correlations with Car Expertise*

| *ROI* | *Cars–Noncars* | *Car Residuals* |
|---|---|---|
| Left FFA1 | .40 (.04) | .41 (.04) |
| Left FFA2 | .33 (.06) | .34 (.06) |
| Left OFA | .11 (.35) | .13 (.32) |
| Left LO | .49 (.01) | .60 (.001) |
| rFFA1 | .01 (.49) | .22 (.19) |
| rFFA2 | .43 (.03) | .42 (.03) |
| Right OFA | .55 (.005) | .55 (.005) |
| Right LO | .36 (.03) | .32 (.05) |

*B. Pearson Correlations with CFMT*

| *ROI* | *Faces–Nonfaces* | *Face Residuals* |
|---|---|---|
| Left FFA1 | −.14 (NA) | −0.12 (NA) |
| Left FFA2 | .34 (.06) | .31 (.08) |
| Left OFA | .20 (.22) | .18 (.24) |
| Left LO | .14 (.26) | .03 (.44) |
| rFFA1 | −.24 (NA) | −.24 (NA) |
| rFFA2 | .24 (.15) | .22 (.16) |
| Right OFA | .29 (.10) | .22 (.16) |
| Right LO | −.31 (NA) | −.20 (NA) |

(A) Correlations between behavioral expertise for cars and neural selectivity for cars using a subtraction and a regression method to control for response to noncar conditions. One-tailed *p* values for positive relations are shown in parentheses. (B) Correlations between behavioral expertise for cars and neural selectivity for cars using a subtraction and a regression method to control for response to noncar conditions. For comparison, we show one-tailed *p* values for positive relations in parentheses. NA = not applicable.



Downloaded from http://direct.mit.edu/jocn/article-pdf/30/7/973/1787628/jocn_a_01256.pdf by guest on 20 September 2021

**Table 3.** Main Task Univariate BOLD Responses (with Standard Error), the Effect Size and $p$ Value for Their Difference (Two-tailed Paired $t$ Test), and the Correlation of the Response to Whole Cars with Car Expertise, Partialing out the Response to Misconfigured Cars

| | *Whole Cars* | *Misconfigured Cars* | | | |
|---|---|---|---|---|---|
| | *Mean (SE)* | *Mean (SE)* | *Cohen's dz* | *p* | *Partial Corr. with Car Exp (95% CI)* |
| lFFA1 | 0.70 (0.09) | 0.60 (0.09) | .27 | .22 | .05 (−.40, .48) |
| lFFA2 | 0.20 (0.06) | 0.05 (0.07) | .50 | .02 | .00 (−.42, .42) |
| lOFA | 1.21 (0.16) | 1.21 (0.14) | .00 | .99 | .07 (−.42, .53) |
| lLO | 0.92 (0.09) | 0.92 (0.07) | .00 | .97 | .26 (−.16, .60) |
| rFFA1 | 1.15 (0.09) | 1.10 (0.08) | .14 | .52 | .14 (−.31, .54) |
| rFFA2 | 0.49 (0.05) | 0.36 (0.04) | .60 | .01 | .20 (−.25, .58) |
| rOFA | 1.66 (0.10) | 1.50 (0.07) | .47 | .05 | .03 (−.52, .56) |
| rLO | 1.37 (0.07) | 1.21 (0.05) | .52 | .01 | .43 (.06, .70) |

participants recruited to vary in car expertise (e.g., coefficient of variation for CFMT: 17.7%, for VET-car: 30.4%; for beta weights for faces in rFFA2: 82%, for beta weights for cars in rFFA2: 132%).

### Univariate Analysis: Sensitivity to Configuration

The mean univariate responses to whole cars and misconfigured car images in each ROI are shown in Table 3. Note that misconfigured cars still have easily recognizable features within each half (although misconfigured, they are not scrambled). Only a subset of the ROIs where car expertise predicted neural activity for cars showed significantly greater responses for whole cars than for misconfigured cars: the left FFA2, rFFA2, and right LO. These effects may represent a nonspecific reduction of activity for misconfigured objects as they were generally not related to car expertise, except in the right LO, where the response to whole cars (partialing out the response to misconfigured cars) was moderately associated with car expertise ($r$ = .43). Because these analyses were exploratory, we only report confidence intervals around effect sizes.

### Multivariate Analyses: Configural Sensitivity

Our primary goal was to investigate whether the FFA would show patterns of responses to car parts that were more similar to the response to misconfigured cars than the response to whole cars, as a function of car expertise. To this end, we first trained a probabilistic SVM (McGugin, Newton, et al., 2014; Chang & Lin, 2011) to distinguish activation patterns elicited by configurally intact whole car images from those elicited by misconfigured car

**Table 4.** Main Task Classification Probabilities and Correlations with Car Expertise

| | *Whole vs. Misconfigured Voxel Patterns* | | *Classification of Combined Voxel Patterns* | | |
|---|---|---|---|---|---|
| | *Probability Correct* | *Correlation with Car Expertise* | *Classified as Whole* | *Correlation with Car Expertise* | |
| | *Mean (SE)* | *r (95% CI)* | *Mean (SE)* | *r (95% CI)* | *p* |
| lFFA1 | 0.62 (0.03) | −.02 (−.46, .43) | 0.52 (0.02) | .18 (−.29, .58) | .54 |
| lFFA2 | 0.59 (0.02) | −.06 (−.47, .37) | 0.50 (0.01) | .04 (−.39, .45) | .89 |
| lOFA | 0.64 (0.02) | .29 (−.22, .68) | 0.51 (0.02) | .32 (−.19, .69) | .23 |
| lLO | 0.60 (0.02) | .14 (−.28, .51) | 0.53 (0.01) | .00 (−.40, .40) | .99 |
| rFFA1 | 0.63 (0.02) | .38 (−.06, .70) | 0.52 (0.02) | −.08 (−.49, .36) | .78 |
| rFFA2 | 0.62 (0.02) | .39 (−.05, .70) | 0.49 (0.01) | .57 (.18, .85) | .01 |
| rOFA | 0.67 (0.02) | .43 (.00, .73) | 0.51 (0.02) | .10 (−.35, .51) | .73 |
| rLO | 0.62 (0.02) | .27 (−.12, .59) | 0.49 (0.01) | .20 (−.19, .54) | .22 |

Downloaded from http://direct.mit.edu/jocn/article-pdf/30/7/973/1787628/jocn_a_01256.pdf by guest on 20 September 2021

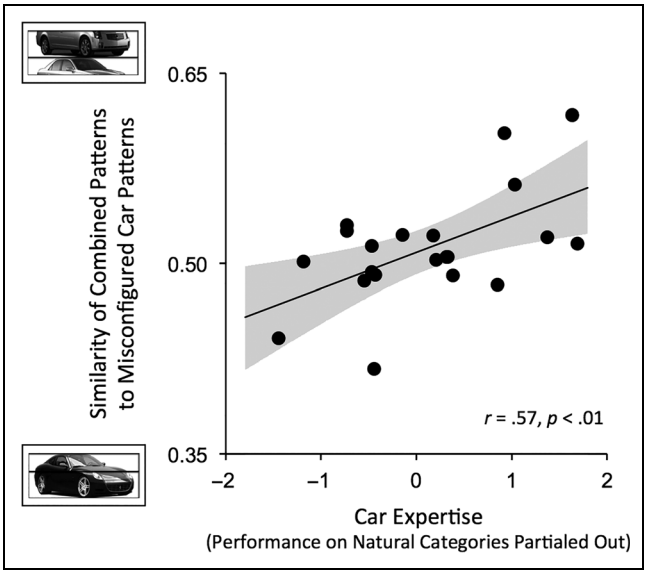


**Figure 2.** Similarity of combined voxel patterns to the voxel patterns elicited by configurally disrupted cars correlated with car expertise. Combined patterns were linear combinations of the voxel patterns elicited by top and bottom car parts when presented in isolation. A probabilistic SVM classifier was trained to discriminate voxel patterns elicited by configurally intact car images from the voxel patterns elicited by configurally disrupted car images (top and bottom halves switched) and tested on combined patterns.

images. Testing the classifier with leave-one-block-out cross-validation revealed above-chance ($p < .05$) classification in all ROIs (Table 4). Just as for the corresponding univariate analysis, we did not have predictions for which ROIs should be better able to classify whole versus misconfigured cars, a fairly easy categorization that all ROIs can perform on average. Because these analyses were exploratory, we only report confidence intervals around effect sizes. Effect sizes were relatively large in the right OFA, rFFA1, and rFFA2.

To test our main hypothesis, we then used the classifier to classify combined patterns (linear combinations of the voxel patterns elicited by top and bottom car parts when presented in isolation). If car expertise is related to sensitivity to configural information, then we would expect that, in participants with greater expertise, the classifier would tend to classify the pattern of activity elicited by the combined patterns as more similar to misconfigured cars and less similar to whole cars. The predicted correlation between expertise and classification of combined patterns as misconfigured was significant in rFFA2 (Table 4, Figure 2).

## DISCUSSION

For the first time, we demonstrate an association between object expertise and configural information represented by multivoxel BOLD activation patterns in rFFA2. As a function of car expertise, representations in this region exhibit sensitivity to configuration—a hallmark of holistic representation—as shown by a classifier's tendency to judge a combined pattern of car parts as less car-like. These findings help to link previous fMRI work demonstrating an increase in univariate BOLD selectivity for objects of expertise with behavioral studies that suggest that experts make greater use of configural information than novices (Chua et al., 2015; Bukach et al., 2010; Wong, Palmeri, & Gauthier, 2009; Wong, Palmeri, Rogers, Gore, & Gauthier, 2009; Gauthier & Tarr, 2002).

In addition, we replicated the previously reported increase in univariate BOLD selectivity to cars relative to other objects in several face-selective areas. As we found previously (McGugin, Newton, et al., 2014; McGugin, Van Gulick, et al., 2014), these effects are distributed among several face-selective regions as well as non-face-selective areas (LO). We demonstrated previously that, of these regions, the rFFA2 is most robust in its relation to experience with cars (McGugin, Van Gulick, et al., 2014) and with faces (McGugin et al., 2017), showing an effect of expertise even under manipulations that abolish the effects in other ROIs. The FFA2 is closer than the FFA1 to an area reported by Nestor, Plaut, and Behrmann (2011), which is not face-selective but codes for face identity, and to even more anterior areas such as the perirhinal cortex, which are important to the representations of complex conjunctions of features (O'Neil, Barkley, & Köhler, 2013). These regions, especially in the right hemisphere, emerge as a network that is important in the creation of more abstract representations of faces, objects, or scenes (Barense, Henson, Lee, & Graham, 2010).

Consistent with our results, a number of recent studies suggested that univariate BOLD selectivity, the original index of selectivity for faces and a standard measure in fMRI studies of expertise, may be too liberal an index of neural selectivity to relate to behavior. For example, univariate BOLD activation to faces is not always sufficient to differentiate patients with developmental prosopagnosia (DP)—a group defined by their below-average face expertise—from controls (Zhang et al., 2015; Avidan et al., 2014; Furl et al., 2011). In other cases, the correlation between behavioral face expertise and univariate BOLD activation has been inconsistent (e.g., Jiang et al., 2013; Pierce, Haist, Sedaghat, & Courchesne, 2004), although as we have discussed, this may sometimes be a function of limited variability in face expertise. In contrast, multivariate measures have shown promise in relating behavioral measures to neural representations in FFA, even in cases where there was no relationship between univariate BOLD activation and expertise (e.g., Zhang et al., 2015; McGugin, Van Gulick, et al., 2014; Jiang et al., 2013).

It is not yet clear why MVPA measures should index expertise effects more reliably than univariate BOLD activation. In some cases, it may be that MVPA simply provides a more sensitive measure (Jiang et al., 2013). In other cases, the results are more qualitatively different (e.g., Zhang et al., 2015; McGugin, Van Gulick, et al., 2014),

Downloaded from http://direct.mit.edu/jocn/article-pdf/30/7/973/1787628/jocn_a_01256.pdf by guest on 20 September 2021

suggesting that there may be substantial heterogeneity of responses across voxels within an ROI (although this variability may not necessarily indicate a multidimensional code; Davis et al., 2014). The approach that we took here was specifically intended to measure the amount of configural information present in the multivoxel pattern of activity extracted from each of our ROIs. A similar measure has been used in the face recognition literature to differentiate patients with DP and controls even in the absence of any differences in univariate BOLD activation (Zhang et al., 2015), in line with behavioral evidence that patients with DP have deficits in configural processing relative to controls (Liu & Behrmann, 2014; Marotta et al., 2002). We should emphasize, again, that car novices are in many ways not comparable with prosopagnosic patients: The contrast between car novices and car experts is more likely quantitative (and indeed we treat expertise as a continuum), whereas there are more striking differences between patients with DP and controls. For instance, congenital prosopagnosia is considered a disconnection syndrome (Avidan et al., 2014), whereas experts in a domain would not be expected to have qualitatively different connectivity between areas compared with novices, Nonetheless, our expectation that the FFA's sensitivity to car configuration as measured via MVPA may be a more stringent test of car expertise is based on these neuropsychological findings, which suggest a general framework in which to understand brain–behavioral relations for patients and controls, for both faces and objects. In addition, our operationalization of a configural representation has a good face validity as it directly relates to behavioral studies that have used similar stimuli and found behavioral effects of expertise (Chua et al., 2015; Bukach et al., 2010; Wong, Palmeri, & Gauthier, 2009; Wong, Palmeri, Rogers, et al., 2009; Gauthier & Tarr, 2002).

In addition to testing the standard correlation between car selectivity and expertise and our main prediction for the combined representations of car parts, we also conducted exploratory analyses of whether car expertise predicted the univariate activity for whole cars (controlling for the response to scrambled cars) and the classifier's ability to decode whole from scrambled faces. We had no clear predictions for these comparisons because they rely on contrasts that should be easily processed even by novices, but we note that, in addition to showing significant or near-significant effects in the FFA, these analyses revealed expertise effects in early areas (the right OFA for MVPA and the right LO for the univariate effect). Although these effects could be due to feedback projections from FFA, prior work suggests that the right OFA is the first area differentiating faces from objects and that it is important in representing parts (Pitcher, Walsh, Yovel, & Duchaine, 2007). It may play a similar role for other categories of expertise, and some work suggests that the representation of parts changes in expertise (Chua et al., 2015). Finally, although it may seem surprising that the domain-general area LOC shows an effect of car expertise, this could also represent tuning with experience of mechanisms that are engaged regardless of expertise. Indeed, this area, rFFA2, and the left FFA2 showed a larger response to whole than misconfigured cars in all participants, consistent with these regions with known sensitivity to scrambling (Grill-Spector, Kushnir, Hender, & Malach, 2000). An interesting and speculative possibility is that the univariate measure is more sensitive than the MVPA to attentional effects, with greater attention increasing the BOLD activation. In support of this suggestion, McGugin, Van Gulick, et al. (2014) reported that correlations between car expertise and mean BOLD selectivity were abolished within FFA and OFA when attention was directed toward a different object (a butterfly), whereas correlations between car expertise and the information content of multivoxel patterns were not affected by redirecting attention (McGugin, Van Gulick, et al., 2014). Indeed, although behavioral expertise typically requires considerable experience, there is evidence that online task demands can increase the univariate BOLD response to nonexpert object categories (Haist, Lee, & Stiles, 2010) and faces from an artificially created in-group (Van Bavel, Packer, & Cunningham, 2011).

In the approach we used here, one consideration is how the response to individual parts should be combined in our combined representations. We used an equal combination of the patterns elicited by a particular part combination, as has been used in some previous work (e.g., MacEvoy & Epstein, 2011). Our results did not depend on this choice, as we found a similar pattern of results when top and bottom parts were weighted 25/75 or 75/25. Baeck, Wagemans, and de Beeck (2013) compared different methods and found that the response to a pair of objects was best predicted by a weighted average of the responses to each object in the pair with a larger weight for the object that elicits a maximal response on its own, although the average response was nearly as effective. Interestingly, when the task required attending to a meaningful configuration between the two objects, the best-weighted average favored the preferred object even more. Although the interaction of task with weighting was not quite significant in Baeck et al., their results suggest that two objects in a pair are weighted differently when their configuration is attended. This raises an interesting interpretation of our expertise effects. Different parts of the same object are meaningfully related, and one theory suggests that attention to diagnostic parts is the change in expertise that can account for holistic effects (Chua et al., 2015). Although all our participants were asked to perform the same task, car experts may be processing cars at the subordinate level regardless of instructions, whereas novices may not (Gauthier, Tarr, Anderson, Skudlarski, & Gore, 1999; Tanaka & Taylor, 1991). Thus, although the results may suggest a different kind of representation in experts, they could also reflect that experts attend to all parts of an object of expertise. However, if this were the case, the correlation between expertise and our configural

Downloaded from http://direct.mit.edu/jocn/article-pdf/30/7/973/1787628/jocn_a_01256.pdf by guest on 20 September 2021

measure ought to reverse when the top and bottom parts were weighted more or less, which we did not observe.

### Limitations

This study has several limitations: One is that we only tested men, so as not to confound expertise and gender. Another is that the limited field of view of high-resolution imaging and the greater field inhomogeneities at 7 T limited the number of face-selective ROIs (for instance, we did not look at face-selective areas in the anterior temporal lobe or early visual cortex). For the same reasons, we do not address issues of connectivity among areas of the face-selective network and the rest of the brain (e.g., Wang et al., 2016).

Although we had enough power to detect moderate effects of expertise, our confidence intervals on these effects are relatively large. Indeed, because we deliberately recruited participants who varied in car expertise, our design would not be ideal to characterize the effect size in the normal population. In addition, because of the difficulty of achieving sufficient power to test differences between correlations of these magnitudes, we should be cautious to draw strong conclusions in comparing across ROIs. For similar reasons, it is not possible to make a strong claim about the multivariate effects being limited to FFA2, but it is still interesting to note that, although the distinction between FFA1 and FFA2 is a relatively new trend in the literature (see Weiner & Grill-Spector, 2010; Pinsk et al., 2009), there is already some emerging evidence that the correlation between univariate BOLD activation and expertise may be more prominent in FFA2 than in FFA1 (McGugin, Newton, et al., 2014; McGugin, Van Gulick, et al., 2014; McGugin, Gatenby, et al., 2012).

### Conclusions

Overall, our results provide further evidence for qualitative changes in object representations in the FFA, especially the rFFA2, as a result of expertise. In addition, they build on behavioral studies associating expertise with an increase in holistic/configural processing recognition (Chua et al., 2015; Bukach et al., 2010; Wong, Palmeri, & Gauthier, 2009; Wong, Palmeri, Rogers, et al., 2009; Gauthier & Tarr, 2002), demonstrating that a similar neural measure also differentiates between car experts and car novices.


### Acknowledgments

This work was funded by the Temporal Dynamics of Learning Center (NSF grant SMA 1041755), NSF SBE 1257098, NEI Training Grant T32 EY07135, and the Vanderbilt Vision Research Center (NEI P30 EY008126).



Reprint requests should be sent to David A. Ross, Department of Psychology, 441 Tobin Hall, University of Massachusetts Amherst, Amherst, MA 01003, or via e-mail: davidross@umass.edu.


### Notes

1. Where expertise effects have not been observed (e.g., Harel et al., 2010; Grill-Spector, Knouf, & Kanwisher, 2004), proposed mediating factors include the specificity of the stimuli (e.g., modern car experts tested with antique cars; Bukach, Phillips, & Gauthier, 2010; Bukach, Gauthier, & Tarr, 2006) and competition between categories of expertise and attentional factors (e.g., McGugin, Van Gulick, Tamber-Rosenau, Ross, & Gauthier, 2014; Harel et al., 2010).
2. Two participants had very low scores on one of the eight VET categories ($z$ scores of $-2.5$ and $-3$). For these participants, we omitted these categories when calculating the nonvehicle aggregate; however, the choice to omit these categories did not change any of the reported findings.

## REFERENCES


Avidan, G., Tanzer, M., Hadj-Bouziane, F., Liu, N., Ungerleider, L. G., & Behrmann, M. (2014). Selective dissociation between core and extended regions of the face processing network in congenital prosopagnosia. *Cerebral Cortex, 24,* 1565–1578.

Baeck, A., Wagemans, J., & de Beeck, H. P. O. (2013). The distributed representation of random and meaningful object pairs in human occipitotemporal cortex: The weighted average as a general rule. *Neuroimage, 70,* 37–47.

Barense, M. D., Henson, R. N., Lee, A. C., & Graham, K. S. (2010). Medial temporal lobe activity during complex discrimination of faces, objects, and scenes: Effects of viewpoint. *Hippocampus, 20,* 389–401.

Bilalić, M., Grottenthaler, T., Nägele, T., & Lindig, T. (2016). The faces in radiological images: Fusiform face area supports radiological expertise. *Cerebral Cortex, 26,* 1004–1014.

Bilalić, M., Langner, R., Ulrich, R., & Grodd, W. (2011). Many faces of expertise: Fusiform face area in chess experts and novices. *Journal of Neuroscience, 31,* 10206–10214.

Bukach, C. M., Gauthier, I., & Tarr, M. J. (2006). Beyond faces and modularity: The power of an expertise framework. *Trends in Cognitive Sciences, 10,* 159–166.

Bukach, C. M., Phillips, W. S., & Gauthier, I. (2010). Limits of generalization between categories and implications for theories of category specificity. *Attention, Perception, & Psychophysics, 72,* 1865–1874.

Chang, C. C., & Lin, C. J. (2011). LIBSVM: A library for support vector machines. *ACM Transactions on Intelligent Systems and Technology (TIST), 2,* 27.

Chua, K.-W., Richler, J. J., & Gauthier, I. (2015). Holistic processing from learned attention to parts. *Journal of Experimental Psychology: General, 144,* 723–729.

Davis, T., LaRocque, K. F., Mumford, J. A., Norman, K. A., Wagner, A. D., & Poldrack, R. A. (2014). What do differences between multi-voxel and univariate analysis mean? How subject-, voxel-, and trial-level variance impact fMRI analysis. *Neuroimage, 97,* 271–283.

Duchaine, B., & Nakayama, K. (2006). The Cambridge Face Memory Test: Results for neurologically intact individuals and an investigation of its validity using inverted face stimuli and prosopagnosic participants. *Neuropsychologia, 44,* 576–585.

Elbich, D. B., & Scherf, S. (2017). Beyond the FFA: Brain–behavior correspondences in face recognition abilities. *Neuroimage, 147,* 409–422.

Friston, K. J., Frith, C. D., Turner, R., & Frackowiak, R. S. (1995). Characterizing evoked hemodynamics with fMRI. *Neuroimage, 2,* 157–165.



Downloaded from http://direct.mit.edu/jocn/article-pdf/30/7/973/1787628/jocn_a_01256.pdf by guest on 20 September 2021

Furl, N., Garrido, L., Dolan, R. J., Driver, J., & Duchaine, B. (2011). Fusiform gyrus face selectivity relates to individual differences in facial recognition ability. *Journal of Cognitive Neuroscience, 23,* 1723–1740.
Gauthier, I., Curran, T., Curby, K., & Collins, D. (2003). Perceptual interference supports a non-modular account of face processing. *Nature Neuroscience, 6,* 428–432.
Gauthier, I., Skudlarski, P., Gore, J. C., & Anderson, A. W. (2000). Expertise for cars and birds recruits brain areas involved in face recognition. *Nature Neuroscience, 3,* 191–197.
Gauthier, I., & Tarr, M. J. (2002). Unraveling mechanisms for expert object recognition: Bridging brain activity and behavior. *Journal of Experimental Psychology: Human Perception and Performance, 28,* 431.
Gauthier, I., Tarr, M. J., Anderson, A. W., Skudlarski, P., & Gore, J. C. (1999). Activation of the middle fusiform "face area" increases with expertise in recognizing novel objects. *Nature Neuroscience, 2,* 568–573.
Gauthier, I., Williams, P., Tarr, M. J., & Tanaka, J. (1998). Training 'greeble' experts: A framework for studying expert object recognition processes. *Vision Research, 38,* 2401–2428.
Golarai, G., Liberman, A., & Grill-Spector, K. (2017). Experience shapes the development of neural substrates of face processing in human ventral temporal cortex. *Cerebral Cortex, 27,* 1229–1244.
Grill-Spector, K., Knouf, N., & Kanwisher, N. (2004). The fusiform face area subserves face perception, not generic within-category identification. *Nature Neuroscience, 7,* 555–562.
Grill-Spector, K., Kushnir, T., Hender, T., & Malach, R. (2000). The dynamics of object-selective attention correlate with recognition performance in humans. *Nature Neuroscience, 3,* 837–843.
Haist, F., Lee, K., & Stiles, J. (2010). Individuating faces and common objects produces equal responses in putative face-processing areas in the ventral occipitotemporal cortex. *Frontiers in Human Neuroscience, 4,* 181.
Harel, A., Gilaie-Dotan, S., Malach, R., & Bentin, S. (2010). Top–down engagement modulates the neural expressions of visual expertise. *Cerebral Cortex, 20,* 2304–2318.
Jiang, X., Bollich, A., Cox, P., Hyder, E., James, J., Gowani, S. A., et al. (2013). A quantitative link between face discrimination deficits and neuronal selectivity for faces in autism. *Neuroimage: Clinical, 2,* 320–331.
Kay, K. N., Weiner, K. S., & Grill-Spector, K. (2015). Attention reduces spatial uncertainty in human ventral temporal cortex. *Current Biology, 25,* 595–600.
Kriegeskorte, N., Goebel, R., & Bandettini, P. (2006). Information-based functional brain mapping. *Proceedings of the National Academy of Sciences, U.S.A., 103,* 3863–3868.
Liu, T. T., & Behrmann, M. (2014). Impaired holistic processing of left–right composite faces in congenital prosopagnosia. *Frontiers in Human Neuroscience, 8,* 750.
MacEvoy, S. P., & Epstein, R. A. (2011). Constructing scenes from objects in human occipitotemporal cortex. *Nature Neuroscience, 14,* 1323–1329.
Marotta, J. J., McKeeff, T. J., & Behrmann, M. (2002). The effects of rotation and inversion on face processing in prosopagnosia. *Cognitive Neuropsychology, 19,* 31–47.
McGugin, R. W., Gatenby, C., Gore, J. C., & Gauthier, I. (2012). High-resolution imaging of expertise reveals reliable object selectivity in the FFA related to perceptual performance. *Proceedings of the National Academy of Sciences, U.S.A., 109,* 17063–17068.
McGugin, R. W., Newton, A. T., Gore, J. C., & Gauthier, I. (2014). Robust expertise effects in right FFA. *Neuropsychologia, 63,* 135–144.
McGugin, R. W., Richler, J. J., Herzmann, G., Speegle, M., & Gauthier, I. (2012). The Vanderbilt Expertise Test reveals domain-general and domain-specific sex effects in object recognition. *Vision Research, 69,* 10–22.
McGugin, R. W., Ryan, K. F., Tamber-Rosenau, B. J., & Gauthier, I. (2017). The role of experience in the face-selective response in right FFA. *Cerebral Cortex,* 1–14. doi:10.1093/cercor/bhx113.
McGugin, R. W., Van Gulick, A. E., Tamber-Rosenau, B. J., Ross, D. A., & Gauthier, I. (2014). Expertise effects in face selective areas are robust to clutter and diverted attention but not to competition. *Cerebral Cortex, 25,* 2610–2622.
Nestor, A., Plaut, D. C., & Behrmann, M. (2011). Unraveling the distributed neural code of facial identity through spatiotemporal pattern analysis. *Proceedings of the National Academy of Sciences, U.S.A., 108,* 9998–10003.
O'Neil, E. B., Barkley, V. A., & Köhler, S. (2013). Representational demands modulate involvement of perirhinal cortex in face processing. *Hippocampus, 23,* 592–605.
Pierce, K., Haist, F., Sedaghat, F., & Courchesne, E. (2004). The brain response to personally familiar faces in autism: Findings of fusiform activity and beyond. *Brain, 127,* 2703–2716.
Pinsk, M. A., Arcaro, M., Weiner, K. S., Kalkus, J. F., Inati, S. J., Gross, C. G., et al. (2009). Neural representations of faces and body parts in macaque and human cortex: A comparative fMRI study. *Journal of Neurophysiology, 101,* 2581–2600.
Pitcher, D., Walsh, V., Yovel, G., & Duchaine, B. (2007). TMS evidence for the involvement of the right occipital face area in early face processing. *Current Biology, 17,* 1568–1573.
Russell, R., Duchaine, B., & Nakayama, K. (2009). Super-recognizers: People with extraordinary face recognition ability. *Psychonomic Bulletin & Review, 16,* 252–257.
Schiltz, C., Dricot, L., Goebel, R., & Rossion, B. (2010). Holistic perception of individual faces in the right middle fusiform gyrus as evidenced by the composite face illusion. *Journal of Vision, 10,* 25.
Schiltz, C., Sorger, B., Caldara, R., Ahmed, F., Mayer, E., Goebel, R., et al. (2006). Impaired face discrimination in acquired prosopagnosia is associated with abnormal response to individual faces in the right middle fusiform gyrus. *Cerebral Cortex, 16,* 574–586.
Talairach, J., & Tournoux, P. (1988). *Co-planar stereotaxic atlas of the human brain*. New York: Thieme.
Tanaka, J. W., & Taylor, M. (1991). Object categories and expertise: Is the basic level in the eye of the beholder? *Cognitive Psychology, 23,* 457–482.
Van Bavel, J. J., Packer, D. J., & Cunningham, W. A. (2011). Modulation of the fusiform face area following minimal exposure to motivationally relevant faces: Evidence of in-group enhancement (not out-group disregard). *Journal of Cognitive Neuroscience, 23,* 3343–3354.
Van Gulick, A. E., McGugin, R. W., & Gauthier, I. (2016). Measuring nonvisual knowledge about object categories: The Semantic Vanderbilt Expertise Test. *Behavior Research Methods, 48,* 1178–1196.
Wang, X., Zhen, Z., Song, Y., Huang, L., Kong, X., & Liu, J. (2016). The hierarchical structure of the face network revealed by its functional connectivity pattern. *Journal of Neuroscience, 36,* 890–900.
Weiner, K. S., & Grill-Spector, K. (2010). Sparsely-distributed organization of face and limb activations in human ventral temporal cortex. *Neuroimage, 52,* 1559–1573.
Wong, A. C. N., Palmeri, T. J., & Gauthier, I. (2009). Conditions for facelike expertise with objects: Becoming a Ziggerin expert—But which type? *Psychological Science, 20,* 1108–1117.
Wong, A. C. N., Palmeri, T. J., Rogers, B. P., Gore, J. C., & Gauthier, I. (2009). Beyond shape: How you learn about

Downloaded from http://direct.mit.edu/jocn/article-pdf/30/7/973/1787628/jocn_a_01256.pdf by guest on 20 September 2021

objects affects how they are represented in visual cortex. *PLoS One, 4,* e8405.
Worsley, K. J., Evans, A. C., Marrett, S., & Neelin, P. A. (1992). Three-dimensional statistical analysis for CBF activation studies in human brain. *Journal of Cerebral Blood Flow & Metabolism, 12,* 900–918.
Xu, Y. (2005). Revisiting the role of the fusiform face area in visual expertise. *Cerebral Cortex, 15,* 1234–1242.
Zhang, J., Liu, J., & Xu, Y. (2015). Neural decoding reveals impaired face configural processing in the right fusiform face area of individuals with developmental prosopagnosia. *Journal of Neuroscience, 35,* 1539–1548.

Downloaded from http://direct.mit.edu/jocn/article-pdf/30/7/973/1787628/jocn_a_01256.pdf by guest on 20 September 2021